



PHYSICS DEPARTMENT OF TURIN
MASTER'S DEGREE COURSE IN PHYSICS

Development and test of FPGA
firmware for the readout of the
ABACUS chip for
beam monitoring applications in
hadron therapy

Academic year 2020/2021

Candidate: Stefan Cristi Zugravel
Supervisor: Dott. Luca Pacher
Co-Supervisor: Prof. Vincenzo Monaco

August 4, 2021

Abstract

Hadron therapy is a particular type of oncological radiotherapy for the treatment of solid tumors that uses proton or ion beams instead of conventional X-rays. The usage of hadron particles allows a better control on the energy release, improving the precision of the treatment and the conservation of healthy tissues around the target. Particle beams are obtained by means of dedicated accelerators, requiring a precise control of particle flux and beam profile. Thus beam-monitoring systems become of primary importance, demanding the usage of fast particle sensors and readout electronics to monitor real-time the particle beam reaching the patient.

In this context the Medical Physics group at University of Torino and INFN (the Italian National Institute for Nuclear and Particle Physics) is participating to the MoVeIT (Modeling and Verification for Ion beam Treatment planning) research project, which aims to develop new and innovative models for biologically optimized Treatment Planning Systems (TPS) using ion beams in hadron therapy. As part of the project the Torino group is involved in the development of solid state detectors and readout electronics for measuring with high precision the characteristics of the hadron beam for irradiation, such as number of particles delivered per unit time, energy and beam profile.

Low-Gain Avalanche Diode (LGAD) thin silicon sensors segmented in strips have been selected as a promising choice for the implementation of the final beam-monitoring system. Thanks to the internal gain mechanism in fact, this sensor technology allows to obtain a large signal-to-noise ratio (SNR) for very low amounts of deposited charge, thus allowing to detect and count single beam particles.

Silicon strips are read out by a full-custom and optimized Application Specific Integrated Circuit (ASIC) designed by Torino INFN. The chip, named ABACUS (Asynchronous-logic-Based Analog Counter for Ultra fast Silicon strips), has been designed using a commercial CMOS 110 nm and integrates 24 readout channels. Each channel includes a low-noise preamplifier and a fast discriminator. The data acquisition system uses commercial Field Programmable Gate Array (FPGA) boards that receive the data from up to six readout chips.

This thesis presents my personal contributions on the upgrade of the FPGA firmware used to characterize the second version of the ABACUS chip and measurement results. The FPGA used to readout the chip is a Kintex-7 KC705 board by Xilinx programmed using the VHDL Hardware Description Language. The FPGA is responsible for both the chip configuration and sensor data readout.

The first part of my work describes the upgraded VHDL firmware, which includes several new features such as: i) the creation of a debugging tool for malfunctioning channels on the board; ii) the complete rewriting of the internal Digital to Analog Converter (DAC) configuration system for the new ABACUS chip, which now uses an address-based system instead of a serial method; iii) the addition of a timestamp in the data packets for a more accurate calculation of the particle rate; iv) the implementation of a latch for internal counters; v) firmware modifications that allow the usage of LVDS (Low-Voltage Differential Signaling) signals instead of CML (Current Mode Logic) ones.

The second part of the thesis presents experimental results for the characterization of

the second version of the ABACUS chip. Measurements include DAC-linearity studies and threshold scans to quantify the threshold dispersion between channels

This thesis is organized as follow:

Chapter 1 describes the physical and biological mechanisms and advantages of hadrontherapy compared to conventional radiotherapy. The most advanced dose distribution systems and the detectors used are described. It also highlights how the use of innovative detectors based on a direct counting mechanism of the individual particles of the beam can be of benefit for innovative therapeutic approaches in the future.

Chapter 2 describes the devices developed within MoVeIT for dose monitoring. In particular, the operating principle of the LGAD sensors used is shown, and their advantages for the application under study. The characteristics of the chip developed by the INFN of Turin for the amplification and discrimination of signals are also described.

Chapter 3 describes the use and operation of an FPGA board, its main components, the hardware description language and the associated work flow.

Chapter 4 describes the core of the thesis work, thus the implementation of the control logic of the internal DACs, **ecc**———. The correct functioning of the VHDL code was verified both with complete simulations in the development environment used and on the board.

Chapter 5 is dedicated to final considerations and possible future developments.

Contents

1	Hadron Therapy	4
1.1	Introduction	4
1.2	Interaction between matter and charged particles	4
1.3	Effects of radiations on biological systems	7
1.4	Dose distribution systems in hadron therapy	10
1.4.1	Passive dose distribution systems	11
1.4.2	Active dose distribution systems	11
1.4.3	Treatment Planning System	11
1.5	Beam monitoring	11
1.5.1	Silicon detectors	11

Chapter 1

Hadron Therapy

1.1 Introduction

The National Cancer Institute define a tumor[1] as “an abnormal mass of tissue that results when cells divide more than they should or do not die when they should”. In a healthy body, cells grow, divide, and replace each other in the body. As new cells form, the old ones die. When a person has cancer, new cells form when the body does not need them. If there are too many new cells, a group of cells, or tumor, can develop. A tumor develops when cells reproduce too quickly. Tumors can vary in size from a tiny nodule to a large mass, depending on the type, and they can appear almost anywhere on the body. There are three main types of tumor:

- **Benign:** These are not cancerous. They either cannot spread or grow, or they do so very slowly. If a doctor removes them, they do not generally return.
- **Premalignant:** In these tumors, the cells are not yet cancerous, but they have the potential to become malignant.
- **Malignant:** Malignant tumors are cancerous. The cells can grow and spread to other parts of the body.

Radiation therapy is the medical use of ionizing radiation to treat cancer. In conventional radiation therapy, beams of X rays (high energy photons) are produced by accelerated electrons and then delivered to the patient to destroy tumour cells. Using crossing beams from many angles, radiation oncologists irradiate the tumour target while trying to spare the surrounding normal tissues. Inevitably some radiation dose is always deposited in the healthy tissues. When the irradiating beams are made of charged particles (protons and other ions, such as carbon), radiation therapy is called hadron therapy[2]. The strength of hadron therapy lies in the unique physical and radiobiological properties of these particles; they can penetrate the tissues with little diffusion and deposit the maximum energy just before stopping. This allows a precise definition of the specific region to be irradiated. The peaked shape of the hadron energy deposition is called Bragg peak and has become the symbol of hadron therapy. With the use of hadrons the tumour can be irradiated while the damage to healthy tissues is less than with X-rays.

1.2 Interaction between matter and charged particles

Charged particles with mass greater than the one of the electron lose energy in matter through ionization. A classic calculation for the energy lost in ionization can be done taking

into account two assumptions:

- the speed of the atomic electron is negligible compared to the one of the incident particle;
- the mass of the incident particle is big in relation to the target mass. This means that the incident particle for each single hit receives a small amount of momentum and thus the direction of flight does not changes.

This hypothesis is valid keeping into consideration that the mass of the electron is 0.51 MeV, a muon has mass 105.6 MeV, for a proton it is 938.2 MeV and for a carbon ion ^{12}C it is 11177.9 MeV.

The classic calculation results in the Bethe-Block formula in equation 1.1 that describes the average energy loss in the target for unit of length, also called stopping power.

$$-\frac{dE}{dx} = 2\pi N_a r_e^2 m_e c^2 \rho \frac{Z}{A} \frac{z^2}{\beta^2} \left[\ln \left(\frac{2m_e \gamma^2 v^2 W_{max}}{W^2} \right) - 2\beta^2 - \delta 2 \frac{C}{Z} \right] \quad (1.1)$$

In equation 1.1:

- N_a : is the Avogadro number;
- r_e : is the classical radius of the electron;
- m_e : is the mass of the electron;
- ρ : target density;
- Z : target atomic number;
- A : target atomic mass;
- W : target average ionization energy;
- z : incident particle charge;
- W_{max} : maximum energy transferred in a collision;
- δ : polarization parameter in target
- c/z : core electrons shielding parameter
- $\beta = v/c$

The stopping power depends by the target mass, atomic number, density and average ionization energy (A , Z , ρ , W). To overcome and eliminate this dependence it was defined the massic stopping power in equation 1.2 that is measured in $\text{MeV}/(\text{g cm}^2)$

$$\delta = -\frac{1}{\rho} \frac{dE}{dx} \quad (1.2)$$

In figure it can be seen the trend of the massic stopping power of a μ^+ passing through a copper layer.

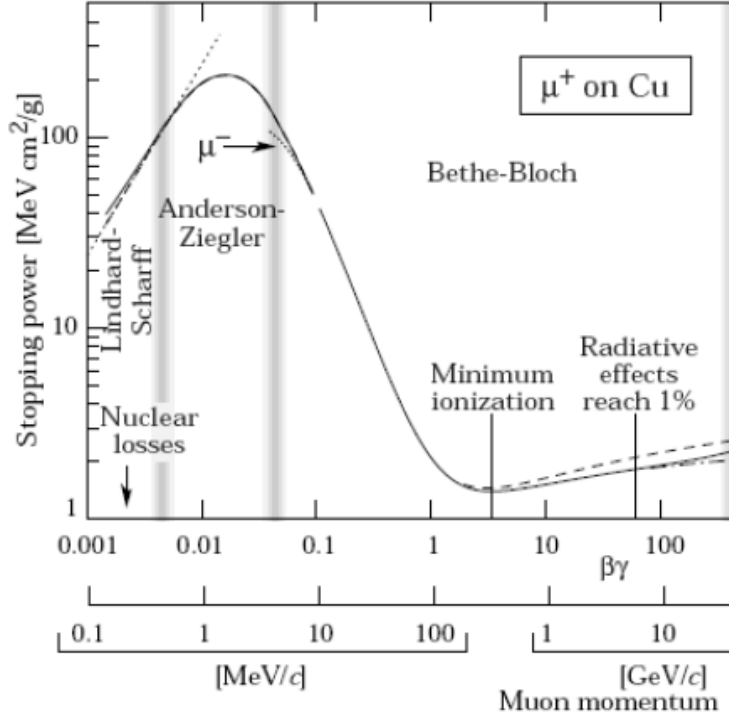


Figure 1.1: Massic Stopping power in function of the μ^+ momentum passing through a copper layer

In the trend of the stopping power in function of the momentum can be noted a de-growth for low momentum values that is due to the term $\frac{1}{\beta^2}$ in equation 1.1; the stopping power decreases until it reaches a minimum, and then slowly grows back.

The average path (range) of a charged particle can be calculated by integrating the stopping power along the "walk".

$$R = \int_{E_i}^0 \frac{1}{\frac{dE}{dx}} dx \quad (1.3)$$

The range depends approximately on the A/Z ratio of the material and grows approximately with the square of the initial kinetic energy of the charged particle. The accrual of energy loss increases as the kinetic energy of the particle decreases with the depth of penetration, with a rapid ascent at the end of the path. The density of ionization of the charged particles along their path in the medium is therefore characterized by a plateau followed by a pronounced maximum towards the end of range, called Bragg peak, which is located at an energy-dependent depth initial kinetics of the incident particle, as shown in figure 1.2. If more particles are considered then it should be kept in mind the statistical fluctuations on the collisions of the particles and on the energy transferred for each collision: these fluctuations are well described by the Landau distribution [3], generate uncertainty about the distance reached by the particles ("straggling"). Beyond all these considerations we must not neglect the possible interactions with the nuclear components of the matter crossed. One effect is enlargement lateral of the beam due to the interaction with the Coulomb fields of the nuclei that it is inversely proportional to the mass of the incident particle. The second effect it is due to the fragmentation of the primary bundle and/or of the nuclei of the material passed through due to nuclear interactions. The fragmentation cross section becomes relevant for ions heavier than the proton, such as carbon ions or heavier, and causes a decrease in the

number of particles incident along the path and the development of secondary fragments. The fragments produced deposit their energy deeper than the Bragg peak giving rise to a queue in the distribution.

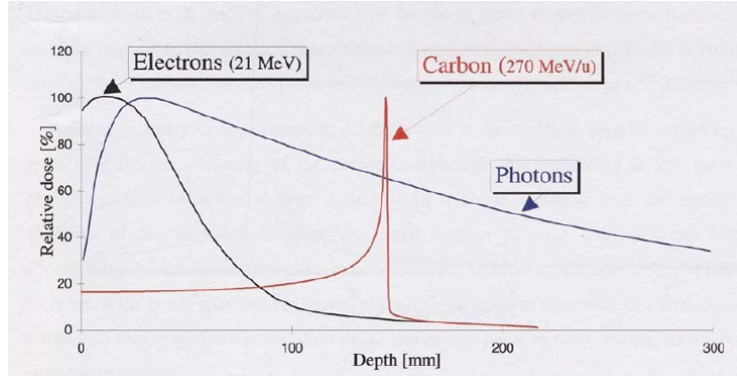


Figure 1.2: Dose profile for a 21MeV electron, 270MeV/u carbon ion and photon beam

1.3 Effects of radiations on biological systems

Radiation is energy. A charged particle when it interacts with the human body loses its energy. The measurement and calculation of the ionizing radiation dose absorbed by an object is called radiation dosimetry.

Thus the dose (D) can be defined as the energy absorbed divided by the object mass.

$$D [Gy] = \frac{dE}{dm} \quad (1.4)$$

In the I.S. the unit of measure is the Gray (Gy) [JKg^{-1}] = $1\text{J}/1\text{Kg}$.

It is also common the use of an equivalent dose ($H = D \times W_1$) where W_1 is a weight that depends on the type of particle (photon, electron, neutron, proton, heavy charged particle, ecc...). The unit of measure of the equivalent dose is the Sievert (Sv) [JKg^{-1}], although in the past it was used the rem [$1\text{Sv} = 100\text{rem}$].

When monitoring the dose absorbed by an human body it must be considered that not every organ has the same resistance to radiation, thus it is used the effective dose ($E = H \times W_2$) which is the equivalent dose multiplied by the weight W_2 which depends on the part of the body interested by the radiations.

The energy deposition is strictly dependent by the type of radiation like photons, electrons or heavy charged particles. As shown in figure 1.2 the relative dose percentage delivered by the photons is maximum at low depth and then has an exponential decrease as the thickness of the tissue increases. The dose profile in function of the depth for heavy charged particles (as carbon ions) is characterized by a low dose at the beginning of the tissue and then by a extremely peaked spike at the end of their travel (Bragg peak). Since the depth of this peak depends by the beam energy, this can be tuned to deliver the dose at different depths. Moreover, thanks to the high mass of the particles, it is possible to greatly reduce the lateral diffusion effects thus saving the healthy tissues and the critical structures near the target.

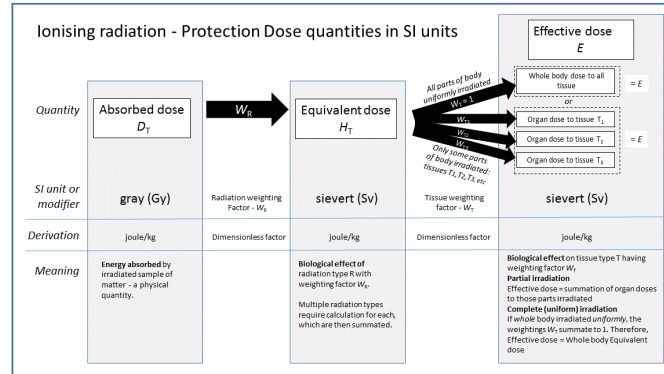


Figure 1.3: Absorbed, equivalent and effective dose units and meanings

With heavy charged particles is therefore possible to accurately focus the beam for a selected depth; this is not possible with other sources of radiation. The different rates of energy loss at different depths for photons and heavy charged particles produce different dose distributions as shown in figure 1.4.

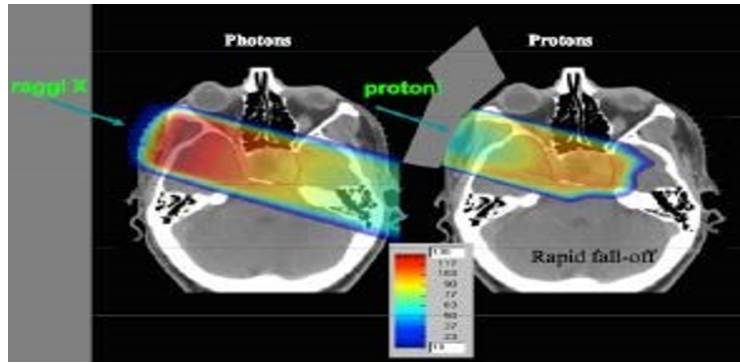


Figure 1.4: Example of a dose distribution for a photon beam on the left and for a proton beam on the right

The energy released by the charged particles can cause both direct and indirect effects. The direct ones are the interactions between the radiation and the biological molecules; this generates breaking points in the nucleotide chain of the DNA. The indirect effects are the interactions, with production of free radicals, between radiations and water molecules inside the cell. After that the free radicals interact with the biological molecules producing chemical alterations that can generate the inactivation of the cell cycle. Damage to DNA molecules is considered the most important since it can lead to the cell's inability to reproduce and cell death[4].

Irradiation can produce various types of alterations in the DNA structure:

- **Single Strand Break (SSB)** when the nucleotide is damaged on a single DNA filament.
- **Double Strand Break (DSB)** when two or more nucleotide are damaged on both DNA filaments.

Following the damage, there are several scenarios:

- **Complete repair**, a situation that occurs for the majority of minor alterations (SSB), after which the cell resumes its normal activity.
- **Wrong repair**, in which the cell repairs its damage but not comprehensively. This can lead to the impossibility of replication of the cell or to its death by apoptosis. In some cases the cell may be able to divide, but by passing on a genetic mutation.
- **Unrepairable damage**, in this scenario the cell dies within a few hours due to the release of lytic enzymes or dies on the occasion of the first mitotic division. This situation occurs mainly in the case of DSB.

The cellular response to radiation depends in a complex way on the absorbed dose. In radiobiology, the biological efficacy of a radiation dose is studied by measuring cell survival as a function of the dose irradiated on the sample. The main physical factor on which biological damage depends, for the same dose administered, is the "Linear Energy Transfer" (LET)[5]:

$$LET = \frac{dE}{dx} \quad (1.5)$$

The LTE is defined as the average ionization density along the trail of a particle and is measured in $\text{keV}/\mu\text{m}$. Radiations with high LET have, considering fixed the absorbed dose, a greater biological effect compared to the ones with low LET. This happens because a higher ionization density imply a greater probability of unrepairable damages, like DSB. The biological effect of a radiation is quantified in terms of Relative Biological Efficiency (RBE), defined as the ratio between the dose required to obtain a specific effect respectively with a reference radiation and with the radiation in question.

$$RBE = \frac{D_{ref}}{D_{test}} \quad (1.6)$$

The reference radiation D_{ref} is commonly represented by a 250 keV X-ray beam, while D_{test} corresponds to the dose of the radiation under examination.

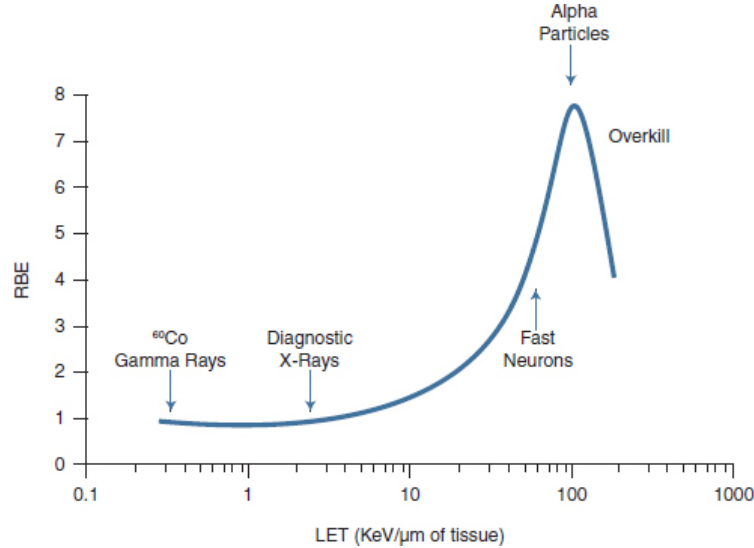


Figure 1.5: RBE in function of the LET

In figure 1.5 it can be seen how the RBE changes in function of the radiation LET. From the graph it can be noted that the RBE growth, in function of the LET, starts for values

near $1 \text{ keV}/\mu\text{m}$ and reaches a maximum near $100 \text{ keV}/\mu\text{m}$. For even higher LET values the RBE decreases, this is caused by a biological saturation effect that happens for high dose (overkill). 10 MeV carbon ions have a LET of $170 \text{ keV}/\mu\text{m}$, this correspond to a RBE of 7. This is one of the reasons why therapies based on the use of carbon ions have been developed, which at the same dose, produce greater biological effects and are more effective in the treatment of radio-resistant tumors.

1.4 Dose distribution systems in hadron therapy

The physical and biological advantages of therapies with charged particles described in the previous paragraphs allow to obtain a precise conformation of the dose to the tumor, while minimizing the risk of side effects due to the irradiation of surrounding healthy organs. These advantages are nowadays exploited in the treatment of delicate tumors in the proximity of organs at risk, pediatric tumors where the risk of side effects must be minimal, and radio-resistant tumors. The number of patients treated with protons or carbon ions is growing each year as it can be seen in figure 1.6

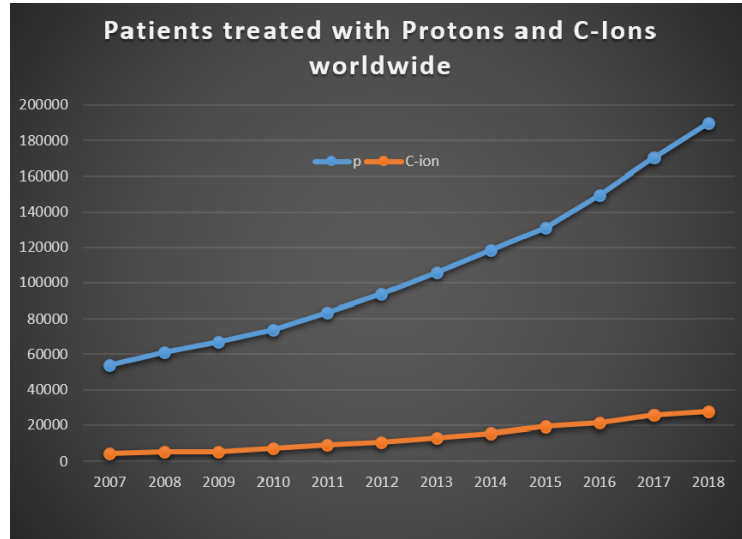


Figure 1.6: Number of patients treated with annually with protons and carbon ions

This numbers, even if are growing, are still a small fraction of the total number of tumors treated with external radiation; X-ray being the main

1.4.1 Passive dose distribution systems

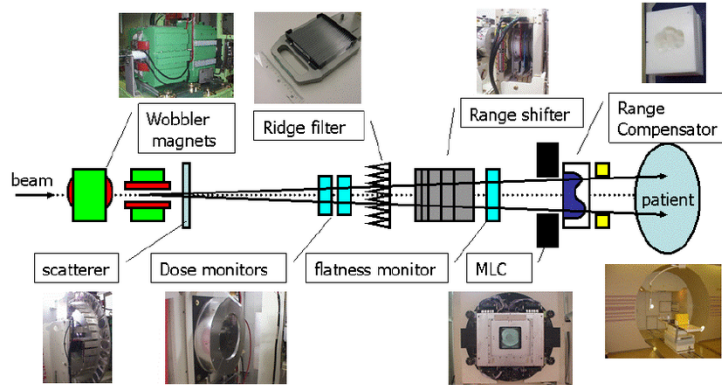


Figure 1.7: Basic design of passive dose distribution system for hadron therapy used to adapt the dose to the form of the tumor

1.4.2 Active dose distribution systems

1.4.3 Treatment Planning System

1.5 Beam monitoring

1.5.1 Silicon detectors

Bibliography

- [1] www.medicalnewstoday.com/articles/249141
- [2] enlight.web.cern.ch/what-is-hadron-therapy
- [3] L. Landau, On the Energy Loss of Fast Particles by Ionization, *Journal of Physics* 8, (1944), 201 -205
- [4] H. Tsujii et al., *Carbon-Ion Radiotherapy – Principles, Practices and Treatment Planning*, Springer, (2012)
- [5] D. Schardt, T. Elsasser, Heavy-ion tumor therapy: Physical and radiobiological benefits, *Reviews of Modern Physics*, 82, (2010)
- [99] Sviluppo su FPGA di tecniche di correzione di effetti d'inefficienza nel conteggio di singoli protoni in fasci terapeutici, Alessio Limardi, 2019-2020.